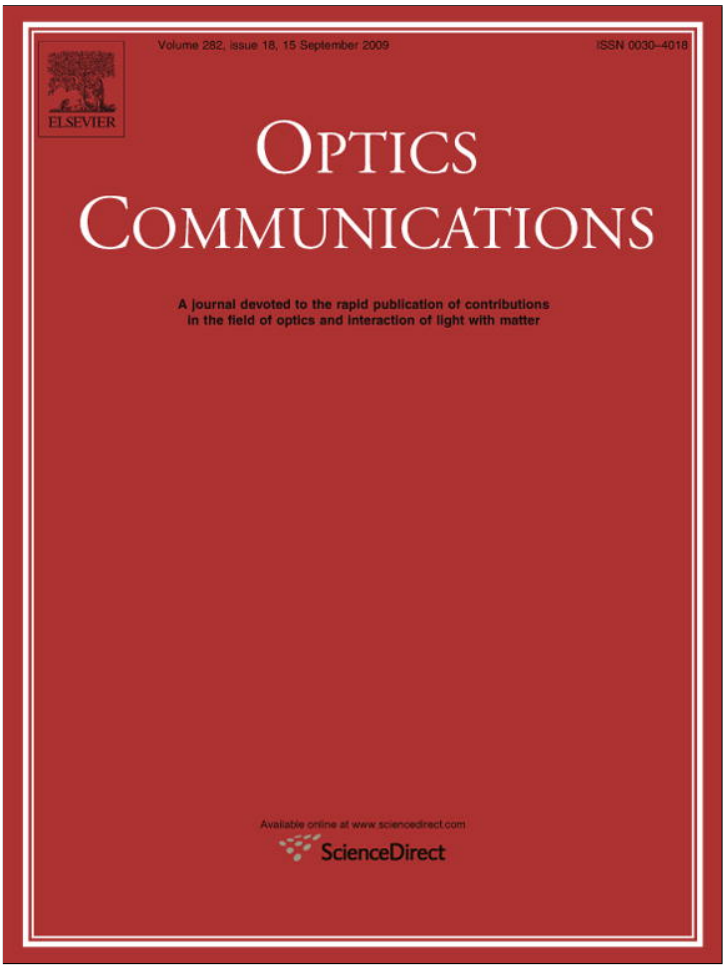

Optics Communications 282 (2009) 3820–3826

Contents lists available at ScienceDirect

Optics Communications

journal homepage: www.elsevier.com/locate/optcom

Eigenvalue system for the scattering from rough surfaces – Saving in computation time by a physical approach

R. Dusséaux [a,*], K. Aït Braham [a], N. Emad [b]

[a] Université de Versailles Saint-Quentin en Yvelines, LATMOS, 10/12 Avenue de l'Europe, 78140 Vélizy, France
[b] Université de Versailles Saint-Quentin en Yvelines, Laboratoire PRiSM, 45 Avenue des Etats-Unis, 78035 Versailles Cedex, France

ARTICLE INFO

Article history:
Received 20 December 2008
Received in revised form 27 May 2009
Accepted 3 June 2009

Keywords:
Scattering from rough surfaces
C method
Eigenvalue system
Beam simulation method
Huygens principle

ABSTRACT

The curvilinear coordinate method is an efficient theoretical tool for analysing rough surfaces. It consists on solving Maxwell's equations written in a nonorthogonal coordinate system. The C method leads to eigenvalue systems and the scattered fields can be expanded as a linear combination of eigensolutions. The boundary conditions allow the combination coefficients to be determined. The dominant computational cost for the C method is the eigenvalue problem solution which is of order of N^3 where N is the size of eigenvalue systems. In this paper, we propose a new approach based on the association of the C method with the beam simulation method (BSM) in order to reduce the computational time. The BSM is based on decomposing a large incident beam into narrower subbeams and then synthesizing the large beam by coherent superposition. The adopted procedure consists of two stages. First, the surface fields are obtained by the C method associated with each elementary beam illuminating smaller surfaces. Second, the total surface field is deduced from a coherent superposition of elementary surface current densities. The far-field and the scattering coefficients are derived from the Huygens principle applied to the total surface fields. We confirm the efficiency and the validity of the approach and show that the BSM applied with the C method allows a significant saving in computation time.

1. Introduction

The curvilinear coordinate method, commonly called the C method, is an efficient theoretical tool for analysing rough surfaces [1–9]. It consists on solving Maxwell's equations under their covariant form written in a nonorthogonal coordinate system which fits the surface profile. The C method leads to eigenvalue systems [1,2]. Then, the scattered fields can be expanded as a linear combination of eigensolutions. The boundary conditions allow the combination coefficients to be determined. The dominant computational cost for the C method is the eigenvalue problem solution which is of order of N^3 where N is the size of the eigenvalue systems.

In a previous work, a new version of the C method based on the short coupling range approximation (SCRA) has been presented and implemented for analysing electromagnetic fields scattered from rough surfaces illuminated by incident monochromatic plane wave [8]. The short coupling range approximation shows that the surface fields at a given point of a rough surface only depend on the shape of the profile inside an interval centered at this point and that has a width of one or two wavelengths of the incident light [10,11]. The new version of the C method consists of two stages. First, according to SCRA, the whole surface is represented by several elementary ones. For each elementary surface, the surface current densities are derived from the C method. Second, the total surface field is deduced from a concatenation of elementary surface current densities and the far-field and the bi-static scattering coefficients are derived from the Huygens principle applied to the total surface fields. In Ref. [8], we have shown that the SCRA applied with the C method allows an important saving in computation time with respect to the C method alone.

In this paper, we propose an extension of this approach to the beam simulation method (BSM) in order to reduce the computational time of the C method. The BSM is based on decomposing a large incident beam into narrower subbeams and then synthesizing the large beam by coherent superposition [12,13]. The adopted procedure also consists of two stages. First, the surface fields are derived from the C method applied to each elementary beam illuminating smaller surfaces. Second, the total surface field is deduced from a coherent superposition of elementary surface current densities and the far-field and the scattering coefficients are derived from the Huygens principle applied to the total surface fields. We confirm the efficiency and the validity of this new approach and show that BSM applied with the C method allows a significant saving in time complexity and consequently in computation time in serial context. The last section is devoted to the parallelism analysis of our technique and brings to light that it is well-suited to parallel computing.

* Corresponding author. Tel.: +33 139254895; fax: +33 139254872.
E-mail address: richard.dusseaux@cetp.ipsl.fr (R. Dusséaux).

0030-4018/$ - see front matter © 2009 Elsevier B.V. All rights reserved.
doi:10.1016/j.optcom.2009.06.010

2. Scattering by random rough surfaces

2.1. Presentation of the problem

We consider a tapered plane wave $F_i(x,y)$ with time dependence $\exp(j\omega t)$ impinging upon a one-dimensional rough surface with a random height profile $y = a(x)$. The surface separates the vacuum (+) from a homogeneous lower medium (−) which can be a dielectric material or perfect conductor. $a(x)$ is a random function whose values obey to a Gaussian probability density with zero mean value and a root-mean-square height h. Its correlation function $C_{aa}(x)$ is also Gaussian with a correlation length l_c.

$$C_{aa}(x) = h^2 \exp\left(-\frac{x^2}{l_c^2}\right) \tag{1}$$

In our previous work [8], we considered a single harmonic plane wave. Here, the plane wave is tapered so that the illuminated zone can be confined to surface L:

$$F_i(x,y) = \frac{1}{2\pi}\int_{-\infty}^{+\infty} \widehat{R}_i(\alpha)\exp(-j\alpha x)\exp\left(+j\beta^{(+)}(\alpha)y\right)d\alpha \tag{2}$$

where

$$\begin{aligned}\widehat{R}_i(\alpha) &= \int_{-\infty}^{+\infty} F_i(x,y=0)\exp(+j\alpha x)dx \\ &= F_0\exp\left(-\frac{b^2}{2}(\alpha-\alpha_i)^2\right)\end{aligned} \tag{3}$$

and

$$\begin{aligned}F_i(x,y=0) &= \frac{1}{2\pi}\int_{-\infty}^{+\infty}\widehat{R}_i(\alpha)\exp(+j\alpha x)d\alpha \\ &= \frac{F_0}{\sqrt{2\pi}b}\exp\left(-\frac{x^2}{2b^2}\right)\exp(-j\alpha_i x)\end{aligned} \tag{4}$$

F_0 is a constant amplitude and $\alpha_i = k^{(+)}\sin\theta_i$, the Gaussian beam axis. b is the parameter that controls the tapering of the incident wave. A Gaussian function $\exp\left(-\frac{u^2}{2\sigma^2}\right)$ is well-described over the range $-3\sigma \leqslant u \leqslant 3\sigma$. So, we consider the length L of the illuminated zone equal to $6b$. $\widehat{R}_i(\alpha)$ is the amplitude associated with the elementary wave function $\exp(-j\alpha x)\exp\left(+j\beta^{(+)}y\right)$. α and $\beta^{(+)}$ are the constant propagations where

$$\alpha^2 + \beta^{(+)2} = k^{(+)2} \quad \text{and} \quad k^{(+)} = \frac{2\pi}{\lambda} \tag{5}$$

λ is the wavelength of the incident wave. For a Gaussian beam, we consider that integration variable α varies from $-\frac{3}{b}+\alpha_i$ to $\frac{3}{b}+\alpha_i$.

Both fundamental polarizations $E_\parallel$ and $H_\parallel$ are considered. In case of $E_\parallel$ polarization, the electric vector is parallel to the Oz axis and for $H_\parallel$ polarization, this is the case of the magnetic vector.

$$\begin{aligned}\vec{E}_i^{(E_\parallel)}(x,y) &= F_i(x,y)\vec{u}_z \\ Z^{(+)}\vec{H}_i^{(H_\parallel)}(x,y) &= F_i(x,y)\vec{u}_z\end{aligned} \tag{6}$$

$Z^{(+)}$ is the intrinsic impedance of free space ($Z^{(+)} = 120\pi$). In the upper medium (+), we note the total field

$$F^{(+)}(x,y) = F_i(x,y) + F_s^{(+)}(x,y) \tag{7}$$

and in the lower dielectric medium (−),

$$F^{(-)}(x,y) = F_s^{(-)}(x,y) \tag{8}$$

The problem consists on working out the field $F_s^{(\pm)}(x,y)$ scattered within the two media.

2.2. The Rayleigh representation of the scattered fields

The scattered field can be expressed by a Rayleigh expansion [14] in the region out of the deformation ($y > \max a(x)$ and $y < \min a(x)$). In case of $E_\parallel$ incident wave we have

$$\begin{aligned}\vec{E}_s^{(E_\parallel,\pm)}(x,y) &= \frac{1}{2\pi}\int_{-\infty}^{+\infty}\widehat{R}^{(E_\parallel,\pm)}(\alpha)\exp\left(\mp j\beta^{(\pm)}(\alpha)y\right)\exp(-j\alpha x)d\alpha\vec{u}_z \\ Z^{(\pm)}\vec{H}_s^{(E_\parallel,\pm)}(x,y) &= \frac{1}{2\pi}\int_{-\infty}^{+\infty}\widehat{R}^{(E_\parallel,\pm)}(\alpha)\left(\frac{\vec{k}_s^{(\pm)}}{k^{(\pm)}}\wedge\vec{u}_z\right)\exp\left(\mp j\beta^{(\pm)}(\alpha)y\right) \\ &\quad\times\exp(-j\alpha x)d\alpha\end{aligned} \tag{9}$$

where

$$\vec{k}_s^{(\pm)} = \alpha\vec{u}_x \mp \beta^{(\pm)}\vec{u}_y \tag{10}$$

$$\alpha^2 + \beta^{(\pm)2} = k^{(\pm)2}; \quad \operatorname{Im}\beta^{(\pm)} < 0 \tag{11}$$

$$k^{(-)} = n^{(-)}k^{(+)} \tag{12}$$

$$Z^{(-)} = \frac{Z^{(+)}}{n^{(-)}} \tag{13}$$

The symbol $\wedge$ designates the vector product. $Z^{(-)}$ is the dielectric medium impedance and $n^{(-)}$, the optical refractive index. $\widehat{R}^{(\pm)}(\alpha)$ is the scattering amplitude associated with the elementary wave function $\exp(-j\alpha x)\exp\left(\mp j\beta^{(\pm)}(\alpha)y\right)$. In the upper medium, if $\left(\alpha \leqslant k^{(+)}\right)$ then $\beta^{(+)}(\alpha)$ is a positive real. The associated wave is an outgoing propagating wave. In the far-field zone, the Rayleigh integral is reduced to the only contribution of these propagating waves and the asymptotic field at an observation point $M(r,\theta)$ is given as follows [15]:

$$\begin{aligned}\vec{E}_s^{(E_\parallel,+)}(r,\theta) &\approx \widehat{R}^{(E_\parallel,+)}\left(k^{(+)}\sin\theta\right)\cos\theta\exp\left(-j\frac{\pi}{4}\right)\frac{\exp\left(-jk^{(+)}r\right)}{\sqrt{\lambda r}}\vec{u}_z \\ Z^{(+)}\vec{H}_s^{(E_\parallel,+)}(r,\theta) &\approx -\widehat{R}^{(E_\parallel,+)}\left(k^{(+)}\sin\theta\right)\cos\theta\exp\left(-j\frac{\pi}{4}\right)\frac{\exp\left(-jk^{(+)}r\right)}{\sqrt{\lambda r}}\vec{u}_\theta\end{aligned} \tag{14}$$

$\vec{u}_\theta$ is the unit vector in the polar coordinate system. In order to obtain the expression of fields in case of $H_\parallel$ polarization, we substitute $\vec{E}_s^{(E_\parallel,\pm)}$ by $Z^{(\pm)}\vec{H}_s^{(H_\parallel,\pm)}$ and $Z^{(\pm)}\vec{H}_s^{(E_\parallel,\pm)}$ by $-\vec{E}_s^{(H_\parallel,\pm)}$ in Eqs. (9) and (14).

The bi-static scattering coefficient $\sigma^{(+)}(\theta)$ is defined from the asymptotic field and represents the angular density of scattered power in the radiation zone normalized with respect to the incident power P_i:

$$\sigma^{(+)}(\theta) = \frac{\cos^2\theta}{2Z^{(+)}P_i}\left|\widehat{R}^{(+)}\left(k^{(+)}\sin\theta\right)\right|^2 \tag{15}$$

where

$$P_i = \frac{1}{4\pi Z^{(+)}}\int_{-\infty}^{+\infty}\left|\widehat{R}_i(\alpha)\right|^2\beta^{(+)}(\alpha)d\alpha \tag{16}$$

In the random rough surface scattering problem, the scattering amplitude $\widehat{R}^{(+)}(\alpha)$ is a random function. So, for a set of N_R surface profiles, we define an averaged bi-static scattering coefficient $\langle\sigma^{(+)}(\theta)\rangle$. The angular bracket $\langle\ \rangle$ stand for ensemble averaging. The coherent intensity corresponds to the bi-static scattering coefficient associated with the averaged scattering amplitude. The incoherent intensity $I_f^{(+)}(\theta)$ is defined as the difference between the two preceding physical quantities

$$I_f^{(+)}(\theta) = \frac{\cos^2\theta}{2Z^{(+)}P_i}\left(\left\langle\left|\widehat{R}^{(+)}\left(k^{(+)}\sin\theta\right)\right|^2\right\rangle - \left|\left\langle\widehat{R}^{(+)}\left(k^{(+)}\sin\theta\right)\right\rangle\right|^2\right) \tag{17}$$

The Monte Carlo technique is applied to estimate the incoherent intensity from the results over N_R different realizations of the profile.

3. Analysis with the curvilinear coordinate method and the Huygens principle

The scattered field cannot be expressed by the Rayleigh expansion inside the modulated zone [14]. In order to overcome this problem, we can obtain an expression of fields that is valid over the surface by solving Maxwell's equations under their covariant form in the translation coordinate system. The curvilinear coordinate method gives the surface current densities and the Huygens–Fresnel principle, the scattering amplitudes.

3.1. Coordinate system – covariant components of field

The translation system is obtained from the Cartesian one (x,y,z) [1].

$$\begin{cases} x' = x \\ y' = y - a(x) \\ z' = z \end{cases} \tag{18}$$

The limit surface $a(x)$ is of equation $y' = 0$ in the translation system. The change from Cartesian components $(V_x; V_y; V_z)$ of vector $\vec{V}$ to covariant components $(V_{x'}; V_{y'}; V_{z'})$ is given by [1,16]

$$\begin{cases} V_{x'}(x;y') = V_x(x;y) + \dot{a}(x)V_y(x;y) \\ V_{y'}(x;y') = V_y(x;y) \\ V_{z'}(x;y') = V_z(x;y) \end{cases} \quad \text{with} \quad \dot{a}(x) = \frac{da}{dx} \tag{19}$$

Covariant components $V_{y'}(x;y')$ and $V_{z'}(x;y')$ become identified with Cartesian components $V_y(x;y)$ and $V_z(x;y)$ where $y' = y - a(x)$. $V_{x'}$ and $V_{z'}$ are parallel to coordinate surfaces $y' = y_0$, so the covariant components $E_{x'}$, $H_{x'}$, $E_{z'}$ and $H_{z'}$ are tangential to the rough surface. In a source-free medium, the Maxwell's equations and the constitutive equations written in the translation system lead to the differential system (20) [2]:

$$\begin{aligned} \frac{j}{k^{(\pm)}}\frac{\partial F^{(\pm)}(x,y')}{\partial y'} &= G^{(\pm)}(x,y') - \dot{a}(x)K^{(\pm)}(x,y') \\ \frac{j}{k^{(\pm)}}\frac{\partial G^{(\pm)}(x,y')}{\partial y'} &= \frac{j}{k^{(\pm)}}\frac{\partial K^{(\pm)}(x,y')}{\partial x} + F^{(\pm)}(x,y') \\ \frac{1}{jk^{(\pm)}}\frac{\partial F^{(\pm)}(x,y')}{\partial x} &= -\dot{a}(x)\Big(G^{(\pm)}(x,y') - \dot{a}(x)K^{(\pm)}(x,y')\Big) + K^{(\pm)}(x,y') \end{aligned} \tag{20}$$

System (20) is valid for the two types of polarization. For $E_\parallel$ polarization, covariant components $F^{(\pm)}(x,y')$, $G^{(\pm)}(x,y')$ and $K^{(\pm)}(x,y')$ are defined as follows:

$$\begin{aligned} F^{(E_\parallel,\pm)}(x,y') &= E^{(\pm)}_{z'}(x,y') \\ G^{(E_\parallel,\pm)}(x,y') &= Z^{(\pm)}H^{(\pm)}_{x'}(x,y') \\ K^{(E_\parallel,\pm)}(x,y') &= Z^{(\pm)}H^{(\pm)}_{y'}(x,y') \end{aligned} \tag{21}$$

and, for $H_\parallel$ polarization, we have:

$$\begin{aligned} F^{(H_\parallel,\pm)}(x,y') &= Z^{(\pm)}H^{(\pm)}_{z'}(x,y') \\ G^{(H_\parallel,\pm)}(x,y') &= -E^{(\pm)}_{x'}(x,y') \\ K^{(H_\parallel,\pm)}(x,y') &= -E^{(\pm)}_{y'}(x,y') \end{aligned} \tag{22}$$

After a Fourier transform, system (20) takes the form:

$$\begin{aligned} \frac{j}{k^{(\pm)}}\frac{\partial \widehat{F}^{(\pm)}(\alpha,y')}{\partial y'} &= \widehat{G}^{(\pm)}(\alpha,y') - \hat{a}(\alpha) * \widehat{K}^{(\pm)}(\alpha,y') \\ \frac{j}{k^{(\pm)}}\frac{\partial \widehat{G}^{(\pm)}(\alpha,y')}{\partial y'} &= \frac{\alpha}{k^{(\pm)}}\widehat{K}^{(\pm)}(\alpha,y') + \widehat{F}^{(\pm)}(\alpha,y') \\ \frac{-\alpha}{k^{(\pm)}}\widehat{F}^{(\pm)}(\alpha,y') &= -\hat{a}(\alpha) * \Big(\widehat{G}^{(\pm)}(\alpha,y') - \hat{a}(\alpha) * \widehat{K}^{(\pm)}(\alpha,y')\Big) + \widehat{K}^{(\pm)}(\alpha,y') \end{aligned} \tag{23}$$

where $\hat{a}(\alpha) * \widehat{V}(\alpha,y')$ is the convolution product of two functions $\hat{a}(\alpha)$ and $\widehat{V}(\alpha,y')$. $\widehat{F}^{(\pm)}(\alpha,y')$, $\widehat{G}^{(\pm)}(\alpha,y')$, $\widehat{K}^{(\pm)}(\alpha,y')$ and $\hat{a}(\alpha)$ are the Fourier transforms of functions $F^{(\pm)}(x,y')$, $G^{(\pm)}(x,y')$, $K^{(\pm)}(x,y')$ and $\dot{a}(x)$, respectively. In a second stage, convolution products are approximated as follows:

$$\begin{aligned} \hat{a}(\alpha) * \widehat{V}(\alpha,y') &= \frac{1}{2\pi}\int_{-\infty}^{+\infty} \hat{a}(\alpha-\gamma)\widehat{V}(\gamma,y')d\gamma \\ &\approx \frac{\Delta\alpha}{2\pi}\sum_{p=-\infty}^{p=+\infty} \hat{a}(\alpha-\alpha_p)\widehat{V}_p(y') \end{aligned} \tag{24}$$

where

$$\alpha_p = p\Delta\alpha \tag{25}$$

and

$$\widehat{V}_p(y') = \widehat{V}(\gamma = \alpha_p, y') \tag{26}$$

$\Delta\alpha$ is the spectral resolution. Finally, substituting expressions (24) into system (23) and applying the point matching method at discrete values $\alpha = \alpha_q$, we obtain:

$$\begin{aligned} \frac{j}{k^{(\pm)}}\frac{\partial \vec{F}^{(\pm)}}{\partial y'} &= [\dot{A}][C][\alpha^{(\pm)}]\vec{F}^{(\pm)} + [C]\vec{G}^{(\pm)} \\ \frac{j}{k^{(\pm)}}\frac{\partial \vec{G}^{(\pm)}}{\partial y'} &= ([I] - [\alpha^{(\pm)}][C][\alpha^{(\pm)}])\vec{F}^{(\pm)} + [\alpha^{(\pm)}][C][\dot{A}]\vec{G}^{(\pm)} \end{aligned} \tag{27}$$

where $[\alpha^{(\pm)}]$ is a diagonal matrix with $\alpha_p/k^{(\pm)}$ along the diagonal, $[I]$ the identity matrix and $[\dot{A}]$ the Toeplitz matrix generated by $\hat{a}(\alpha_q)$ such that its (q,p) element is $\hat{a}(\alpha_q - \alpha_p)$ and

$$[C] = ([I] + [\dot{A}][\dot{A}])^{-1} \tag{28}$$

With a Mth-order truncated approximation, $[\alpha^{(\pm)}]$, $[I]$, $[\dot{A}]$ and $[C]$ are square matrices of dimension M_s where $M_s = 2M + 1$. The upper vector $\vec{F}^{(\pm)}$ and the lower vector $\vec{G}^{(\pm)}$ have components $\widehat{F}^{(\pm)}(\alpha_p,y')$ and $\widehat{G}^{(\pm)}(\alpha_p,y')$ where $-M \leqslant p \leqslant +M$. The elementary solutions of (27) are defined as follows:

$$\begin{pmatrix} \vec{F}^{(\pm)}_n \\ \vec{G}^{(\pm)}_n \end{pmatrix} = \begin{pmatrix} \vec{f}^{(\pm)}_n \\ \vec{g}^{(\pm)}_n \end{pmatrix} \exp\left(-jk^{(\pm)}r^{(\pm)}_n y'\right) \tag{29}$$

with

$$r^{(\pm)}_n \begin{pmatrix} \vec{f}^{(\pm)}_n \\ \vec{g}^{(\pm)}_n \end{pmatrix} = \begin{bmatrix} [\dot{A}][C][\alpha^{(\pm)}] & [C] \\ ([I] - [\alpha^{(\pm)}][C][\alpha^{(\pm)}]) & [\alpha^{(\pm)}][C][\dot{A}] \end{bmatrix} \begin{pmatrix} \vec{f}^{(\pm)}_n \\ \vec{g}^{(\pm)}_n \end{pmatrix} \tag{30}$$

$\vec{f}^{(\pm)}_n$ and $\vec{g}^{(\pm)}_n$ represent the upper eigenvector and the lower eigenvector associated with the eigenvalue $r^{(\pm)}_n$. We write $f^{(\pm)}_n(\alpha_p)$ and $g^{(\pm)}_n(\alpha_p)$ the components of vectors $\vec{f}^{(\pm)}_n$ and $\vec{g}^{(\pm)}_n$, respectively. System (30) gives $2M_s$ eigensolutions. According to the sampling theorem [6,7], the elementary wave functions $\widehat{F}^{(\pm)}_n(\alpha,y')$ and $\widehat{G}^{(\pm)}_n(\alpha,y')$ can be constructed from samples $f^{(\pm)}_n(\alpha_p)$ and $g^{(\pm)}_n(\alpha_p)$ by the following interpolations:

$$\begin{aligned} \widehat{F}^{(\pm)}_n(\alpha,y') &= \sum_{q=-M}^{q=+M} f^{(\pm)}_n(\alpha_q)\mathrm{sinc}\Big(\frac{\pi}{\Delta\alpha}(\alpha-\alpha_q)\Big)\exp\left(-jk^{(\pm)}r^{(\pm)}_n y'\right) \\ \widehat{G}^{(\pm)}_n(\alpha,y') &= \sum_{q=-M}^{q=+M} g^{(\pm)}_n(\alpha_q)\mathrm{sinc}\Big(\frac{\pi}{\Delta\alpha}(\alpha-\alpha_q)\Big)\exp\left(-jk^{(\pm)}r^{(\pm)}_n y'\right) \end{aligned} \tag{31}$$

3.2. Surface fields with the C method

Elementary wave functions $\widehat{F}_n^{(\pm)}(\alpha,y')$ and $\widehat{G}_n^{(\pm)}(\alpha,y')$ characterize an outgoing wave propagating with no attenuation if $\mathrm{Re}\left(\pm k^{(\pm)}r_n^{(\pm)}\right)>0$ and $\mathrm{Im}\left(\pm k^{(\pm)}r_n^{(\pm)}\right)=0$. For an evanescent wave, $\mathrm{Im}\left(\pm k^{(\pm)}r_n^{(\pm)}\right)<0$. For each medium, it is observed numerically that among the $2M_s$ eigenfunctions, M_s of them correspond to outgoing waves and as many to incoming waves. The covariant components of the scattered fields are defined by the following Fourier transforms:

$$\begin{aligned}\widehat{F}_s^{(\pm)}(\alpha,y') &= \sum_{n=1}^{2M+1} A_n^{(\pm)}\widehat{F}_n^{(\pm)}(\alpha,y')\\ \widehat{G}_s^{(\pm)}(\alpha,y') &= \sum_{n=1}^{2M+1} A_n^{(\pm)}\widehat{G}_n^{(\pm)}(\alpha,y')\end{aligned} \tag{32}$$

According to (31) and (32), we obtain in the spatial domain:

$$\begin{aligned}F_s^{(\pm)}(x,y') &= \sum_{n=1}^{2M+1} A_n^{(\pm)}F_n^{(\pm)}(x,y')\\ G_s^{(\pm)}(x,y') &= \sum_{n=1}^{2M+1} A_n^{(\pm)}G_n^{(\pm)}(x,y')\end{aligned} \quad \text{for} \quad |x| \leqslant \frac{2\pi}{\Delta\alpha} \tag{33a}$$

$$F_s^{(\pm)}(x,y') = G_s^{(\pm)}(x,y') = 0 \quad \text{for} \quad |x| > \frac{2\pi}{\Delta\alpha} \tag{33b}$$

The surface fields are given by functions $F_s^{(\pm)}(x,y')$ and $G_s^{(\pm)}(x,y')$ at $y'=0$. The combination coefficients $A_n^{(\pm)}$ are found by solving the boundary conditions according to the type of the lower medium (perfect conductor or dielectric medium) and the polarization of the impinging wave [6].

3.3. Scattering amplitudes derived from the C method and the Huygens principle

As shown in Ref. [8], in the upper medium, the far-field angular dependences are derived from the surfaces fields $F_s^{(\pm)}(x,y'=0)$ and $G_s^{(\pm)}(x,y'=0)$ given by the C method.

$$\begin{aligned}\widehat{R}^{(p,+)}\left(k^{(+)}\sin\theta\right)\cos\theta = \frac{1}{2}\int_{-\pi/\Delta\alpha}^{+\pi/\Delta\alpha}\Big[&(\cos\theta-\dot{a}(x)\sin\theta)F_s^{(p,+)}(x,y'=0)\\ &+G_s^{(p,+)}(x,y'=0)\Big]\times\exp\left(jk^{(+)}\sin\theta x\right)\exp\left(jk^{(+)}\cos\theta a(x)\right)dx\end{aligned} \tag{34}$$

Letter p designates the polarization ($p=E_{\parallel}$ or $p=H_{\parallel}$). The formula (34) is obtained from the Huygens principle associated with the Weyl representation of the zeroth-order Hankel function and the Rayleigh expansion [8]. The curvilinear coordinate method gives the surface fields and the far-field angular dependence is calculated using Eq. (34). The bi-scattering coefficient is given by Eq. (15).

4. The beam simulation method (BSM)

The BSM consists on decomposing a large incident beam. So, function $F_i(x,y=0)$ is decomposed as follows:

$$F_i(x,y=0) = \sum_{q=1-N_b}^{N_b-1} D_{i,q}F_{i,q}(x,y=0) \tag{35}$$

where

$$D_{i,q} = \frac{F_0}{\sqrt{2\pi}b}\exp\left(-\frac{x_q^2}{2b^2}\right) \tag{36}$$

and

$$F_{i,q}(x,y=0) = \exp(-j\alpha_i x)\,\mathrm{tri}\left(\frac{x-x_q}{2c}\right) \tag{37}$$

Local function $\mathrm{tri}\left(\frac{x-x_q}{2c}\right)$ is one triangle of unit amplitude, of width $2c$ and centered on $x_q=qc$:

$$\mathrm{tri}\left(\frac{x-x_q}{2c}\right) = \begin{cases}1 & \text{for } |x-x_q|<c\\ 0 & \text{elsewhere}\end{cases} \tag{38}$$

The incident beam is represented by $2N_b-1$ elementary beams $F_{i,q}(x,y)$ illuminating the plane $y=0$ on a length L/N_b where $L=2N_bc$. In the spectral domain, elementary beams are represented by the Fourier transform of function $F_{i,q}(x)$:

$$\widehat{R}_{i,q}(\alpha) = FT\left[F_{i,q}(x,y=0)\right] = c\,\mathrm{sinc}^2\left(\frac{c(\alpha-\alpha_i)}{2}\right)\exp\left(+j(\alpha-\alpha_i)x_q\right) \tag{39}$$

where $\mathrm{sinc}(\alpha)=\frac{\sin(\alpha)}{\alpha}$. For the numerical implementation, we only consider the main lobe of function sinc^2, where the constant propagation α varies from $\alpha_i-\frac{2\pi}{c}$ to $\alpha_i+\frac{2\pi}{c}$. Substituting (39) in (2), the tapered plane wave $F_i(x,y)$ is given as follows:

$$F_i(x,y) = \sum_{q=1-N_b}^{q=N_b-1} D_{i,q}F_{i,q}(x,y) \tag{40}$$

where

$$F_{i,q}(x,y) = \frac{1}{2\pi}\int_{-\infty}^{+\infty}\widehat{R}_{i,q}(\alpha)\exp(-j\alpha x)\exp\left(+j\beta^{(+)}(\alpha)y\right)d\alpha \tag{41}$$

The curves of Fig. 1 represent the Fourier transforms of the original and synthesized beams in the plane $y=0$ for a configuration characterized by $\alpha_i=30^\circ$, $L=40\lambda$, $N_b=4$ and $c=10\lambda$. As shown in Fig. 1, the beam synthesis method is efficient.

The BSM is based on decomposing a large incident beam into narrower subbeams and then synthesizing the large beam by coherent superposition. In this approach, the scattering of waves by the rough surface with each small beam is independent and is without coherent wave interaction. So, the C method is used to perform the surface fields $F_{s,q}^{(\pm)}(x',y'=0)$ and $G_{s,q}^{(\pm)}(x',y'=0)$ associated with each elementary profile $a_q(x)$ of length $2c+2l_t$ with:

$$\begin{aligned}a_q(x) &= a(x) \quad \text{for } |x-x_q| \leqslant c+l_t\\ a_q(x) &= 0 \quad \text{elsewhere}\end{aligned} \tag{42}$$

The illuminated zone of elementary profile $a_q(x)$ is represented by interval $x_q-c \leqslant x \leqslant x_q+c$. So, elementary profile $a_q(x)$ is illuminated by an elementary narrow beam over a length $2c$. But, in

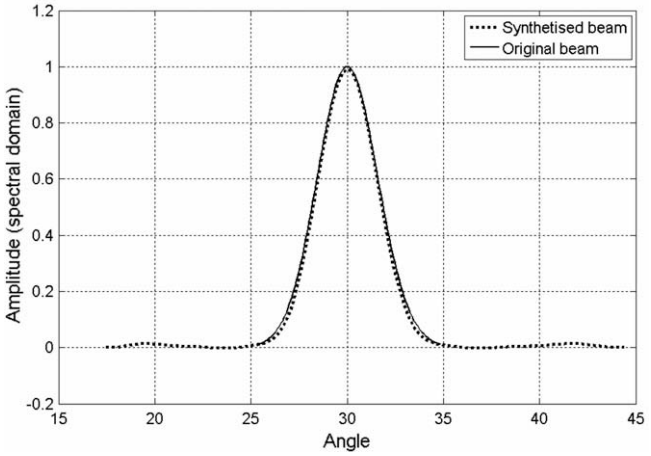

Fig. 1. Original beam and synthesized beam. Simulation parameters: $L=40\lambda$, $N_b=4$ and $\theta_i=30^\circ$.

order to analyze the electromagnetic coupling between the illuminated zone and the one that is not illuminated, we consider elementary profiles $a_q(x)$ defined over $x_q - c - l_t \leqslant x \leqslant x_q + c + l_t$ where length l_t defines a transition zone that is not directly illuminated by the subbeam. According to the short coupling range approximation, this transition zone has a width of one or two wavelengths of the incident light [10,11]. As shown in Fig. 2, two consecutive elementary profiles present a common zone having a length $c + 2l_t$ but they are illuminated by different narrow beams.

The total surface field is deduced from a coherent superposition of elementary surface current densities as follows:

$$\begin{aligned} F_s^{(\pm)}(x, y' = 0) &= \sum_{q=1-N_b}^{q=N_b-1} D_{i,q} F_{s,q}^{(\pm)}(x, y' = 0) \\ G_s^{(\pm)}(x, y' = 0) &= \sum_{q=1-N_b}^{q=N_b-1} D_{i,q} G_{s,q}^{(\pm)}(x, y' = 0) \end{aligned} \tag{43}$$

where $F_{s,q}^{(\pm)}(x, y' = 0) = G_{s,q}^{(\pm)}(x, y' = 0) = 0$ for $|x - x_q| > c + l_t$.

In final, the scattered amplitude is calculated using the total surface fields (43) into Eq. (34) and the bi-static scattering coefficient $\sigma^{(+)}(\theta)$ is given by (15).

5. Numerical results

5.1. Numerical parameters

The spectral resolution $\Delta\alpha$ and the truncation order M are the two numerical parameters of the C method. The spectral resolution is inversely proportional to the deformation length and the truncation order gives the number of unknowns. The analysis of a rough dielectric surface requires the solution of two $2M_s$-dimensional eigenvalue systems and for each polarization, the solution of a linear $2M_s$-dimensional system when dealing with the boundary conditions. The dominant computational cost for the C method is the eigenvalue problem solution which is of the order of N^3 (where $N = 2M_s$ and $M_s = 2M + 1$).

In the spectral domain, the Mth-order truncation removes the highest spatial frequencies of the field components and of the associated eigenwaves. Indeed, integration variable α varies within interval $[-\alpha_{\max}; +\alpha_{\max}]$ where $\alpha_{\max} = M\Delta\alpha$. The proportion of evanescent waves becomes larger when $\alpha_{\max}$ increases, leading to a better description of the coupling phenomena and a better accuracy on results. The higher spatial frequency $\alpha_{\max}$ increases with the increasing of the root-mean-square slope [3,6].

The accuracy on results depends on the value of the highest spatial frequency $\alpha_{\max}$. In order to compare the C method and the C method associated with the BSM, we should give the same value of $\alpha_{\max}$ for both approaches and the same spatial resolution Δx. If we consider two transition zones, the length of the profile treated by the C method alone is $L + 2l_t$. The BSM applied with the C method leads to $2N_b - 1$ eigenvalue systems and treats profiles having a length equal to $\frac{L}{N_b} + 2l_t$. So, the time complexity required with respect to the C method alone is divided by the theoretical factor ρ_{th} given by:

$$\rho_{th} \approx \frac{N_b^3}{2N_b - 1} \left(\frac{L + 2l_t}{L + 2N_b l_t} \right)^3 \tag{44}$$

This saving in time complexity is only due to our physical approach which consists in using BSM in conjunction with the C method rather than this last one alone. (The time complexity represents the number of basic operations of a method or algorithm.) While, the time complexity is independent of the hardware support and the programming language, the computation time which is measured on a given computer depends on these factors. For the simulations presented in this paper, the curvilinear coordinate method and the beam simulation method have been implemented in Matlab language on Xeon-Pentium-3.4 GHz-bi-processor PC with 4 GB RAM. As in this paper our main goal is to valid the proposed approach we have chosen Matlab language and a single computer like programming environment leading to a relatively limited number of realizations. In order to point out the efficiency and stability of our approach for several thousands of realizations, we target in a future work to implement the proposed approach in a high level language (FORTRAN or C++) for a large-scale distributed environment.

5.2. Validation of results

We consider a single realization with a length $L = 48\lambda$ and illuminated under the incidence $\theta_i = 20°$. The rough surface rms height is $h = 0.4\lambda$, the correlation length is $l_c = \lambda$. The optical refractive index is fixed at $n_- = 2.8 - 0.25j$. We choose $N_b = 6$. The Gaussian beam is decomposed into 11 elementary beams illuminating smaller surfaces of length 8λ. Fig. 3 shows the real part of the current surface density $G_s^{(\pm)}(x, y' = 0)$ for the $E_{\parallel}$-polarized configuration and $F_s^{(\pm)}(x, y' = 0)$ for the $H_{\parallel}$-polarized case, respectively. Comparison between surface currents derived from both versions of the C method is good in the $E_{\parallel}$ polarization and satisfactory in

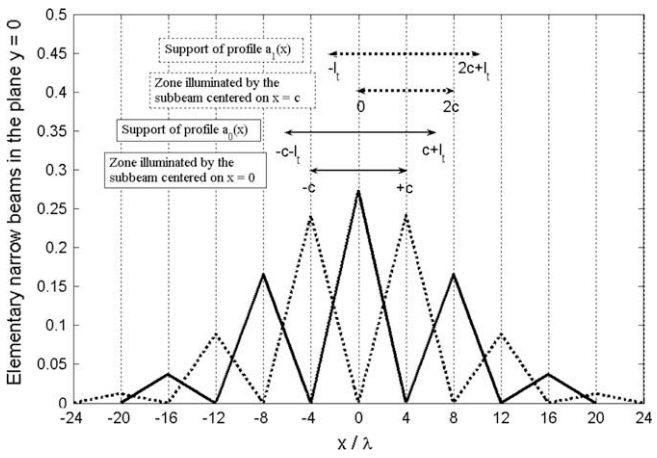

Fig. 2. Elementary narrow beams in the plane $y = 0$. Simulation parameters: $L = 48\lambda$, $N_b = 6$, $\theta_i = 0°$, $c = 4\lambda$ and $l_t = 2\lambda$.

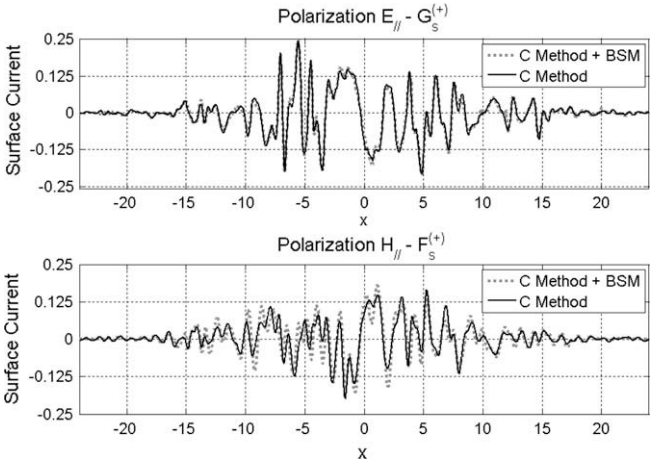

Fig. 3. Real part of surface currents for one realization. Simulation parameters: $L = 48\lambda$, $N_b = 6$, $h = 0.4\lambda$, $l_c = \lambda$, $l_t = 3\lambda/2$, $n_- = 2.8 - 0.25j$, $\theta_i = 20°$, $M^C = 240$, $M^{C\cup BSM} = 51$ and $\alpha_{\max} = 4.7k_+$.

the $H_{\parallel}$ case. The CPU time required for solution of eigenvalue systems in this example is 13 s for the BSM and 121 s for the C method alone, a factor-of-9.3 difference. The theoretical factor ρ_{th} of reduction is equal to 9.1. The total CPU time for the surface fields is 17.2 s for the BSM and 129 s for the C method alone, a factor-of-7.5 difference.

Figs. 4 and 5 give the bi-static coefficient for the same realization. Comparison is conclusive. Nevertheless, we can observe light differences on results that we can explain by an analysis of wave interactions. The C method analyzes all electromagnetic coupling while the BSM does not take into account some wave coherent interactions insofar as the scattering of waves by the rough surface with each elementary beam is independent.

Fig. 6 gives the incoherent intensity $I_f^{(+)}$ obtained by the new version of the C method for a glass interface ($n_- = 1.5$) illuminated by a $H_{\parallel}$-polarized incident plane wave at $\theta_i = 40°$. Results are estimated over 300 realizations. The rough surface rms height is $h = 0.2\lambda$ and the correlation length is $l_c = 0.5\lambda$. We choose $N_b = 6$ and the Gaussian beam is decomposed into 11 elementary beams illuminating smaller surfaces of length 8λ. The length of transition zones is $l_t = 3\lambda/2$. We compare results with the scattering pattern given by a rigorous method based on solutions of surface integral equations [17]. Comparison is conclusive and confirms the validity

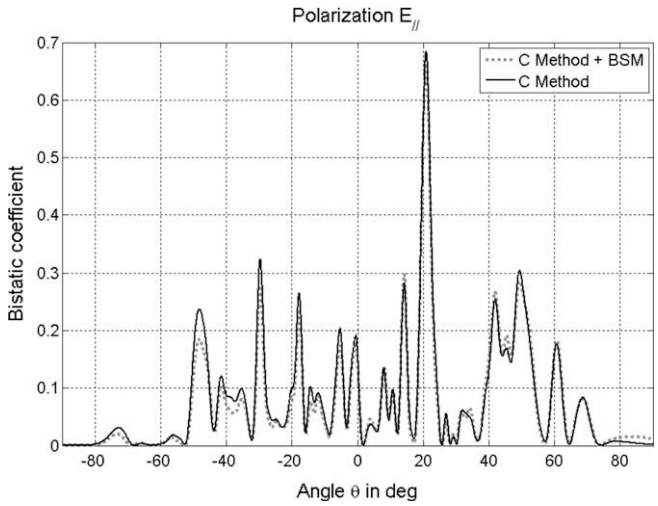

Fig. 4. Bi-static scattering coefficient for one realization under $E_{\parallel}$ polarization. The parameters are those of Fig. 3.

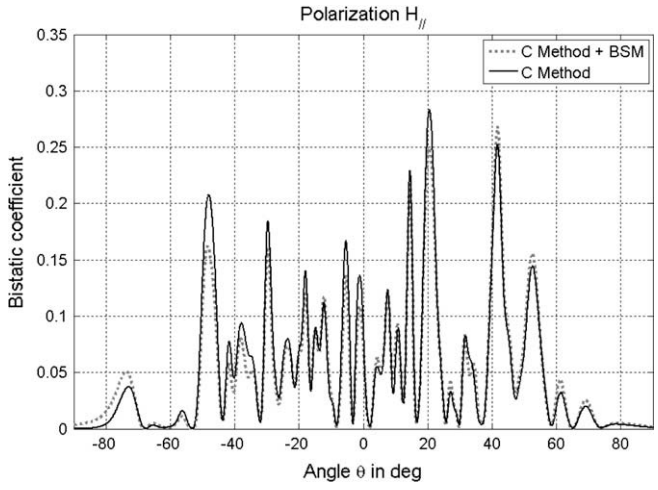

Fig. 5. Bi-static scattering coefficient for one realization under $H_{\parallel}$ polarization. The parameters are those of Fig. 3.

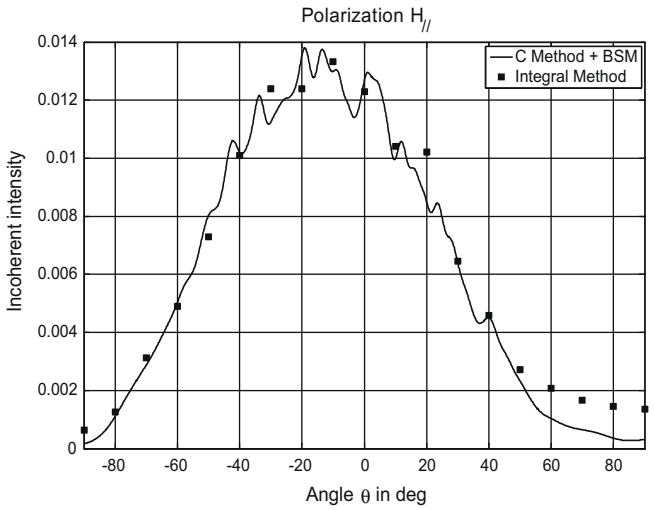

Fig. 6. Incoherent intensity for a glass interface illuminated by a $H_{\parallel}$-polarized incident plane wave. Simulation parameters: $L = 48\lambda$, $N_b = 6$, $h = \lambda/5$, $l_c = \lambda/2$, $l_t = 3\lambda/2$, $n_- = 3/2$, $\theta_i = 40°$, $M^{C_JBSM} = 51$ and $\alpha_{max} = 4.7k_+$. Results of the integral method are taken in Ref. [17].

of BSM approximation for the rough surface under consideration. When increasing the rms slope given by $h_{\dot{a}} = \sqrt{2}h/l$, the radiation is more pronounced in the backscattering region and decreases in the forward direction. For the surface under study, the enhanced backscattering phenomenon is observed, as seen in Fig. 6. The Monte–Carlo simulations based on the new version of the C method have been successful in predicting backscattering enhancement.

6. Parallelism analysis

We have seen that the computation of surface fields by using the C method in conjunction with BSM allows reducing the computing time of the C method. In order to study very large surfaces, an additional option is to exploit the potential parallelism of these methods. Indeed, parallel computing operates on the principle that large problems can be divided into smaller ones, which can be solved in parallel. The good management of the communication and synchronization between these subtasks allows obtaining good parallel program performances such as substantial gain of execution time. To parallelize an algorithm we have to focus on its kernel which is the part of the algorithm which contains most of calculation.

The analysis of a rough surface with the C method requires the solution of two N-order eigenproblems. These problems constitute the kernel of the C method. We have seen that with N large, the proportion of evanescent waves becomes larger leading to a better description of the coupling phenomena and a better accuracy on results. We need to compute all eigenvalues of a large and sparse matrix. The most currently used method allowing this computation is QR algorithm which the computation cost is of order N^3 [18]. In order to improve the performances of the QR algorithm, we can parallelize it. Nevertheless, the exploitation of the parallelism of this algorithm is a delicate task. Indeed, in each of iteration of QR only two rows and two columns of the matrix participate to computation imposing a parallel algorithm with a small degree of parallelism. The reduction in the computation time cannot be substantial.

The C method associated with the beam simulation method (BSM) is based on decomposing a large incident beam into narrower subbeams and then synthesizing the large beam by coherent superposition. The corresponding computation process consists of two main steps. At first, the curvilinear coordinate method determines

the surface fields for each elementary beam illuminating small surfaces. Second, the total surface field is computed by making use of a coherent superposition of elementary surface current densities. Then, the far-field and the scattering coefficients are derived from the Huygens principle applied to the total surface fields. The kernel of this computing process is its first step. That means that the dominant part of the algorithm, in point of view of computation, is the solving of a number of eigenproblems of small or moderate size. A combination of the solution of these problems will determine the total surface fields. This approach is particularly well adapted to large-scale parallel and distributed architectures. Indeed, in the context of a distributed system comprising a network of machines, each of the problems could be solved on a machine whose architecture can be single or multiple processors. The communication of the intermediary results between these machines will then form the solution associated with the total surface fields. The C method associated with BSM has a significant degree of coarse grain parallelism and requires little communication. In addition, the fine grain parallelism of each small or moderate-size eigenproblem could also be exploited. These features offer, by reducing dramatically the computation time, the possibility of studying of very large surface fields by using the C method in conjunction with BSM in a parallel computing context.

7. Conclusion

In this paper, a new version of the C method based on the beam simulation method has been presented and implemented for analysing the electromagnetic field scattered from a one-dimensional random surface. We have shown the efficiency and the validity of BSM for penetrable media in both fundamental polarizations. The BSM applied with the C method allows the analysis of large surfaces and an important saving in computation time with respect to the C method alone. Moreover, we have seen that this approach is particularly well-suited to large-scale distributed systems.

References

[1] J. Chandezon, D. Maystre, G. Raoult, J. Opt. 11 (1980) 235.
[2] L. Li, J. Chandezon, J. Opt. Soc. Am. (1996) 2247.
[3] R. Dusséaux, R. de Oliveira, PIER 34 (2001) 63.
[4] G. Granet, K. Edee, D. Felkacq, PIER 37 (2002) 235.
[5] R. Dusséaux, C. Baudier, PIER 37 (2002) 289.
[6] C. Baudier, R. Dusséaux, K.S. Edee, G. Granet, Waves Random Media 14 (2004) 61.
[7] K. A Braham, R. Dusséaux, G. Granet, Waves Random Complex Media 18 (2008) 255.
[8] K. A Braham, R. Dusséaux, Opt. Commun. 281 (2008) 5504.
[9] K. Edee, B. Guizal, G. Granet, A. Moreau, J. Opt. Soc. Am. A 25 (2008) 796.
[10] D. Maystre, IEEE Trans. Antennas Propag. 31 (1983) 885.
[11] D. Maystre, J.P. Rossi, J. Opt. Soc. Am. 3 (1986) 1276.
[12] M. Saillard, D. Maystre, J. Opt. 19 (1988) 173.
[13] D. Maystre, M. Saillard, J. Ingers, Wave Random Media 1 (1991) 143.
[14] G. Voronovich, Wave Scattering from Rough Surfaces, Springer, Berlin, 1994.
[15] C. Baudier, R. Dusséaux, PIER 34 (2001) 1.
[16] J.A. Stratton, Electromagnetic Theory, McGraw-Hill, New York, 1941.
[17] O. Calvo-Perez, A. Sentenac, J.J. Greffet, Radio Sci. 34 (1999) 311.
[18] G. Golub, C. Van Loan, Matrix Computation, second ed., The John Hopkins University Press, 1989.